CrossMark

ORIGINAL PAPER

Lessons Learned from the Landslides in Shengli East Open-Pit Mine and North Open-Pit Mine in Xilinhot City, Inner Mongolia Province, China

Fan Yongbo · Li Shihai · Zhou Yang ·
Fan Zhiyong · Liu Xiaoyu

Abstract The locations of the 2013 eastern ShengLi open pit mine landslide and the 2010 northern ShengLi open pit mine landslide were both in the XilinHot city of Inner Mongolia province, in areas with similar geographical, regional geological, geomorphic conditions and excavation depth. There are so many similar characteristics, such as landslides triggered by the rain storms, landslides occurred many times, landslides with long time deformation, but there are also some differences between the two landslides, such as the scale and failure mode. Field investigations showed that the two landslides were both occurred several days after the rain storms, the eastern ShengLi open pit mine landslide body with the volume of 85 million m^3 has been in persistent deformation with an observed maximum horizontal displacement of 58 m in August 2013, Furthermore the implemented check dams at east open pit mine had not formed an efficacious blocking system to resist the flow because of incorrect judgment regarding the landslide style. The northern ShengLi open pit mine landslide body with 0.5–1 million m^3 occurred several times after each rain storm. In the whole, the time of persistent deformation about the eastern ShengLi open pit mine was much longer than that of the northern ShengLi open pit mine because of the difference of the filling material of fault and space combination between the faults and the slope. Field investigation, physical model experiments, real-time displacement monitoring and numerical simulation were implemented to investigate the characteristics, mechanism, and retaining measures of the two landslides. The insights gleaned herein may be valuable for the understanding of the mechanisms of landslides and improving preventative measures against these types of events in north China in the future.

Keywords Landslide · Fragmented flowing failure · Fault and filling materials · Xilinhot city

1 Introduction

Landslides are defined as downward and outward movement of slope-forming materials composed of natural rock, soils, artificial fills, and combinations of these materials (Varnes 1958). They generally take place under the influence of common geologic, topographic, or climatic factors. They always trigger more property loss than any other geologic hazards (Varnes 1984). Moreover, much of the damage and a considerable proportion of the loss of life occurring with earthquakes and intense storms have been due to landslides (Cruden 1991; Qi et al. 2006; Zhou et al. 2010; Hitoshi et al. 2010; Wang 2013a, 2014).

F. Yongbo (✉) · L. Shihai · Z. Yang ·
F. Zhiyong · L. Xiaoyu
Key Laboratory for Mechanics in Fluid Solid Coupling Systems, Institute of Mechanics, Chinese Academy of Sciences, Beijing 100190, People's Republic of China
e-mail: ybfan@imech.ac.cn

Springer

The moving mass is proceeding by any one or combination of three principle types of movement: falling, sliding, or flowing (Varnes 1958). The landslide of east open pit mine discussed in this paper was a complex one, with both sliding and flowing. Complex flow-like landslides (CFLLs, Panek 2013; Cuomo 2014) are characterized by an upper section of rocks with a structure that is unfavorably oriented and lower sections composed of earth flows that originate due to liquefaction of material.

On August 16, 2013, a catastrophic landslide occurred following a storm in east open pit mine, Xilinhot City in northern China's Inner Mongolia Province (Fig. 1). The corresponding landslide was approximately 1.62 km long with an area of 1.696 km^2 and a volume of 85 million m^3. According to records taken at the Xilinhot Rainfall Station, the daily rainfall reached 43.5 mm. In response to this high-intensity rainfall event, the catastrophic landslide occurred and destroyed one-fourth of the east open pit mine. Five landslides have occurred in this area during the past three years. On August 31, 2011, the other landslide occurred following a storm in north open pit mine. The corresponding landslide was approximately 0.408 km long with an area of 0.13 km^2 and a volume of 1.1 million m^3. Three landslides have occurred in north open pit mine during the past 4 years.

This paper presents the results of an in-depth study of the deformation characteristics and triggering mechanism of the two landslides via comprehensive geomorphic analysis, tectonic conditions and analysis of observational data. The development tendency of their deformation is also assessed.

Table 1 Parameters of the material in experiment

Type	Cohesion (kPa)	Internal friction angle (°)
Clay	0	31.2
Fine sand	0	25.5
Coarse sand	0	40.6

Table 2 Parameters of the material in numerical simulation

Type	Cohesion (kPa)	Internal friction angle (°)
Bedrock	200	45
Structure surface	0	3
Geological material above the structure surface	20	8

Fig. 1 The location of the two coalmines in Inner Mongolia Province, China

2 Materials and Methods

2.1 Study Area

2.1.1 Geomorphic Conditions

The orientation of the east and north open pit mine are both northeast-southwest. The location of the two open pit mines is 10 km east and 7 km north from Xilinhot City in the eastern part of the Inner Mongolia Plateau. They are both in the transition zone between the denudation-accumulation terrain and low and hilly terrain. The elevation of the two open pit mines is respectively 990–1108 and 800–980 m.

2.1.2 Geological Conditions

The axis of the ShengLi syncline passes through the two open pit mines, the trend of the faults are almost N60°E here. According to the geological investigation data, the F68 fault (N60°E/NW 54°) is waterproof, which plays an important role in the slope stability of the east open pit mine. The F1 (N40°–62°E/SE∠70°) and F25 (N20°–55°E/SE∠50–70°) fault passes through the north open pit mine, the inclination of the F1 and F25 fault is contrary to the inclination of slope.

Strata from top to bottom are Quaternary, the Cenozoic Tertiary Pliocene, and Mesozoic Cretaceous. Coal resources are mainly embedded in the Mesozoic Cretaceous formation.

2.1.3 Hydrological Conditions

The study area has an annual average precipitation of 289 mm. The maximum and minimum recorded yearly rainfall between 1974 and 1980 was 481.0 and 146.7 mm, respectively (Shu 2009). The rainfall is largely concentrated during the period from June to August. On average, 70 % of the annual precipitation is during this period (Fig. 2). Annual average evaporation is 1850 mm. Rock fissure water and Quaternary pore water is the main types of groundwater.

#### 2.1.4 The History of Slope Deformation

Deformation of the east open pit mine appeared on February 3, 2011 with a 130 m long crack and partial dislocation exceeding 20 cm. A landslide occurred on
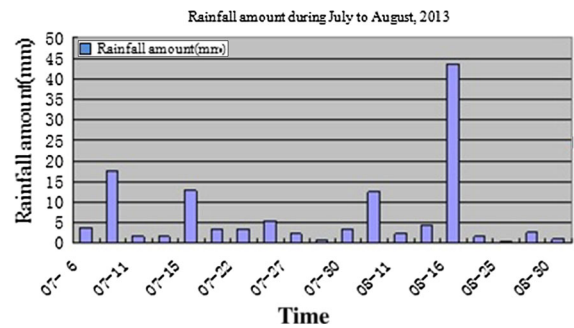
Fig. 2 Rainfall amount during July to August (XiLinHot 2013)

a platform at the elevation of 912–948 m on August 22, 2011. The corresponding landslide had a volume of 1.2 million m^3 and was approximately 320 m long and 180 m wide. On November 7, 2011, a small-scale landslide with a volume of 0.4 million m^3 occurred on a platform at the elevation of 912–948 m. Since then, arc-shaped crack bands I and II appeared. On July 28, 2012, a small-scale landslide with a volume of 0.6 million m^3 occurred again on a platform at the elevation of 900 m. On August 16, 2012, a large-scale landslide with a volume of 20 million m^3 occurred on a platform at the elevation of 912–1056 m after a heavy rainstorm, and the corresponding landslide was approximately 800 m long and 500 m wide. On August 16, 2013, a large-scale landslide with a volume of 85 million m^3 occurred after a heavy rainstorm (daily rainfall of 43.5 mm), and the corresponding landslide was about 1620 m long and 1800 m wide. Since then, the arc-shaped crack band II ran through to the rear of the study area. During the past five landslides, four landslides have occurred in July or August, and the volume of these four landslides was larger than that occurred on November 7, 2011, which indicated that the landslides were connected with the rain storm. Figure 3a illustrates that the velocity of the monitoring points within the deformation area have increased for a long period of time after the landslide. Moreover, the velocity of upper point was less than the lower point, which indicates that the driving force of the landslide originated from the lower part. Figure 3b illustrates that the velocities of the monitoring points within the landslide area have the same characteristics, but the data below the elevation of 924 m is larger than that above the elevation of 924 m.

The east slope of north open pit mine formed in March, 2005, a large area of rock fall at the middle of

(a) **The velocity of monitoring point within deformation area**

(b) **The velocity of monitoring point within landslide area**
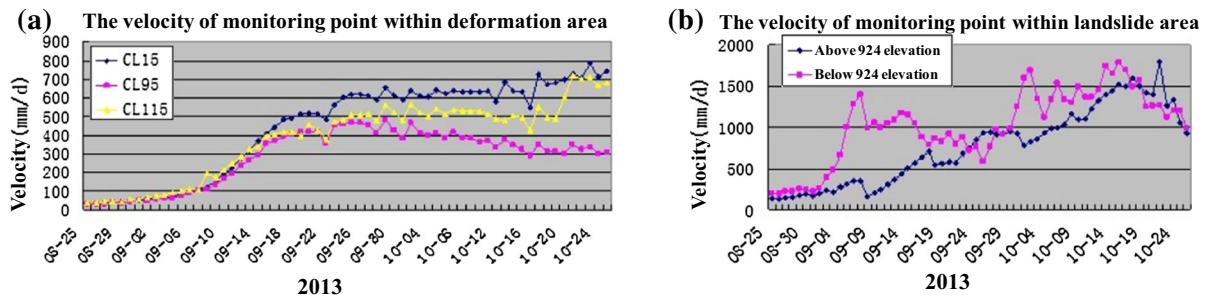
Fig. 3 The velocity of monitoring points within deformation and landslide area about the east open pit mine

the slope occurred in May, 2005. In September and October, 2006, two small-scale landslides occurred in the east slope of north open pit mine. In August, 2007, a large-scale landslide with a volume of 2 million m³ occurred in the south part of the east slope. On August 31, 2011, the corresponding landslide had a volume of 1.0 million m³ occurred in the middle part of the east slope, and was approximately 408 m long and 200 m wide. It has the same characteristics with the east open pit mine, two large landslides have occurred in August.

2.2 Materials

2.2.1 The Mechanism of the Landslide

According Shu (2009), the internal friction angle of Quaternary strata, mudstone, and coal of the east open pit mine were all greater than 20°. The internal friction angle of the weak interlayer was 10° and the dip angles of the slope and strata were 18° and 6–10°. According Sun et al. (2008) and Qu et al. (2009), the internal friction angle of the mudstone in saturation and weak interlayer of the north open pit mine were 25° and 6°–20°, and the dip angles of the slope and strata were 16°–24° and 0°–14°. The two slopes should have good stability if there are not any other influencing factors.

On the other hand, the F68 fault played an important role in the stability of the slope of the east open pit mine. It was a normal fault, and the trend and the dip angle was N60°E/NW 54°. Fault gouge of the F68 was mainly composed of quartz, kaolinite, and illite, so it was hydrophilic and impermeable. Under these geological conditions, the water would infiltrate via the surface cracks and concentrate near to the F68 fault. According to the exploration data, the depth of the groundwater here was 40 m. The water pressure

softened the soil, destroyed the slope structure, and pushed the soil forward and upward. Then, the soil and water mixture washed out of the overlying strata, and the fragmented flowing failure formed. As long as there was constant influx of water, the deformation and failure would continue.

Combination relationship of stratum, fault and slope orientation determined the stability of the slope. Fault gouge of the F1 and F25 was mainly composed of mudstone, carbonaceous mudstone, siltstone, mud-conglomerate. The inclination of the F1 and F25 fault was contrary to the inclination of slope and cut through at the foot of the slope, which had little effect on the stability of the east slope of the north open pit mine. The thickness of the sand soil strata and the clay strata of the north open pit mine was respectively 20 and 10 m, and carbonaceous mudstone with a thickness 70 m was located below the clay, so groundwater usually concentrated here easily because of the low permeability of the clay strata. Thus, the landslide likely occurred through sand soil strata.

#### 2.2.2 The Characteristics of the Two Landslides

2.2.2.1 Similar Characteristics of Long-Term and High-Rate Deformation
Although several landslides have occurred, the deformation of the two slopes is still ongoing. Cumulative lateral displacement of the east open pit mine has reached 60 m. The deformation rate has remained at more than 10 mm per day. The maximum was more than 1 m per day.

The width of the crack at the rear of the north open pit mine is close to 1 m, the maximum of the crack dislocation exceeds 1.5 m. The two slopes have characteristics of a particularly long-term and high-rate deformation.

2.2.2.2 Difference of Fragmented Flowing Failure

The failure of the east open pit mine started near to the F68 fault, and the damage zone gradually extended upward. Based on the GPS data, the velocity and direction of the lateral displacement near the monitoring points was inconsistent, although these points were uniformly located in the deformation area. This indicated that it was not a landslide with one particular slip surface, but a fragmented flowing failure. Below the F68 fault, the surface of slope was extremely flat with slight oscillatory motion, similar to a fluid. The length of the flat fragmented flowing landslide exceeded 600 m, as illustrated in Fig. 4. The landslide was different from the traditional retrogressive or pushing landslides.

2.2.3 Check Dams and Measures on Site

A check dam is here defined as a dam constructed for the purpose of preventing the flow at the foot of a slope (Chanson 2004; Zeng et al. 2009). At the beginning of Nov. 2011, the construction of check dams began at the elevations of 936, 960, and 984 m of the east open pit mine. Due to the influence of the groundwater and the settlement at the 936 m elevation, construction was interrupted and the check dam could not be completed. After several months, the material of the check dam began to slide to the elevation of 900 m following a landslide. On October 2, 2012, check dams
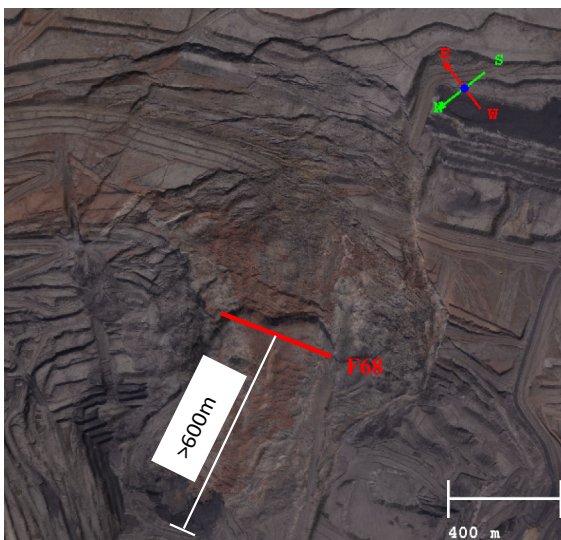
Fig. 4 Fragmented flow failure of the east open pit mine

were constructed once more at the elevations of 924 and 984 m. However, these also ended in failure, as illustrated in Fig. 5.

Monitoring measures included GPS points, SSR radar, and total station, which ensured the continuity and accuracy of the monitoring data. GPS points were distributed in the deformation area, between crack I and crack II (Fig. 6). In addition, cutting and restraining at the top and bottom of the landslide was adopted, simultaneously. Before the rainy season, cracks with width exceeding 10 cm would be filled with mudstone. To some extent, these measures mitigated the deformation speed of the slope, but deformation continued.

Reinforcement project such as anchor cable, slide-resistant pile, and grouting are all not suitable for the north open pit mine because of the surface loose sand and mudstone, rainfall penetrated through the sand strata and concentrated in the mudstone strata, which seriously affected the stability of the slope. According to the combination and thickness of the strata, 116 draining wells carried out in 2011 ensured the stability of the slope. Simultaneously, the management of seepage water from the slope effectively avoided the soaking of the mudstone strata.

3 Results and Discussion

3.1 Experiment and Numerical Simulation About the East Open Pit Mine

3.1.1 Physical Model Experiment

According to the strata structure, strata lithology, geometric features, and boundary conditions of the east open pit mine, a physical model experiment was conducted. The model included three sections: weak strata, upper-stratum, and lower-stratum. Weak strata represented mudstone and the water-bearing stratum, implemented with coarse sand; the water permeability of the upper-stratum was relatively weak, implemented with fine sand; and the lower-stratum was impermeable, implemented with clay to simulate (Table 1). The angle of the strata and the slope were 6° and 18°, respectively. The F68 fault was impermeable, implemented with clay to simulate, and the dip angle was 54°. A water tank was placed at the rear of the slope, and a rectangular opening with 3 × 6 cm

Fig. 5 Collapse of check dams about the east open pit mine
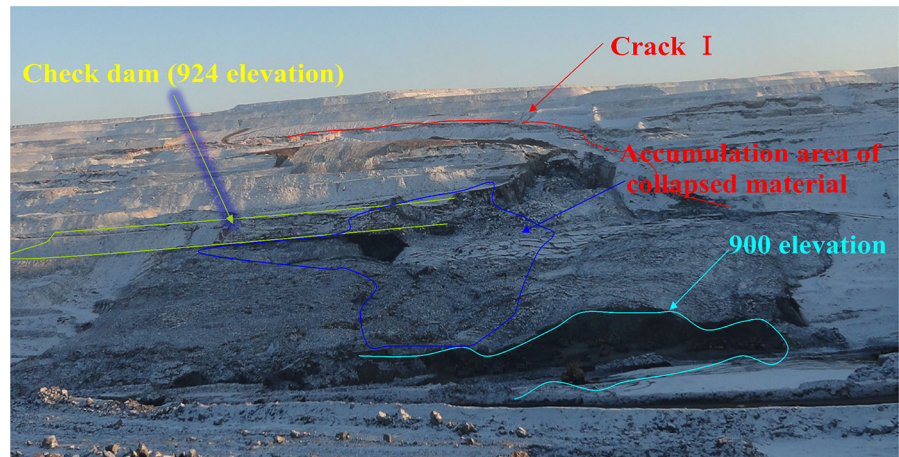
was at the bottom of the water tank, and a pipe filled with coarse sand was connected with the water tank and coarse sand strata, which was used to simulate that water penetrated into the slope body. The profile of the slope and the processing of the landslide were illustrated in Figs. 7 and 8.

3.1.2 Analysis of Experimental Results

Physical model experiments have been used to solve specific problems involving landslides in the last few decades (Wang and Sassa 2003; Huang et al. 2008; Acharya et al. 2009). The failure process of the slope below the F68 fault is summarized as (a) water accumulation, (b) fragmented destruction, and (c) flowing. The experiment revealed that the water permeated from the tank at the end of the slope. Although there were many cracks at the rear of the slope, a pushing landslide did not occur. In fact, the soil near the F68 fault was damaged at first in the experiment, which was consistent with the actual landslide. We conjectured that the water permeated through the coarse sand quickly and concentrated near to the F68 fault in actual landslide. The kaolinite, illite, and other minerals blocked the water so that the water pressure rose rapidly, which resulted in the damage to the soil near the F68 fault. Under the condition of a continuing water supply, the damage to the soil near the F68 fault aggravated and enlarged upward. Simultaneously, fragmented flowing failure occurred below the F68 fault. To some extent, the physical model experiment recreated the dynamic evolution process of the landslide and clarified the relationship between strata structure, the environment, and

transportation of the groundwater. The experimental phenomena were almost consistent with the landslide itself.

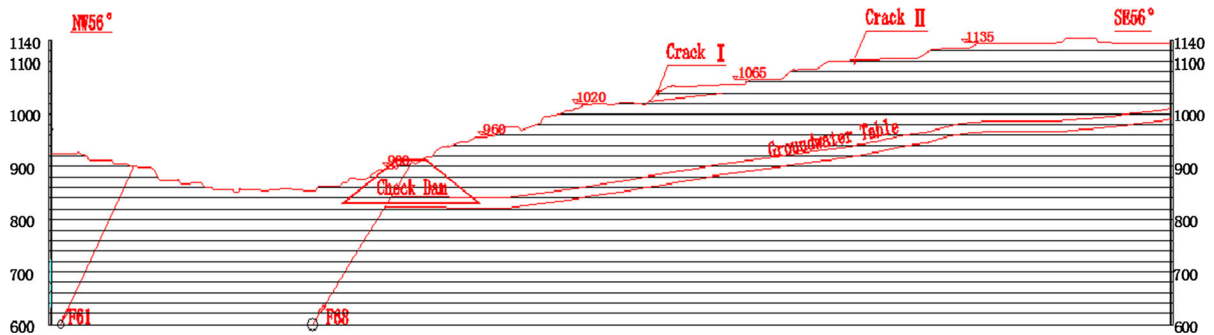### 3.1.3 The Introduction of the Numerical Simulation

3.1.3.1 Introduction of Continuum-Based Discrete Element Method (CDEM)
All of the numerical calculations were done using the continuum-based discrete element method (CDEM), (Li 2013; Feng et al. 2014; Wang et al. 2015; Wang 2013b). The method, which couples FEM and DEM, performs FEM calculation in a single block and conducts DEM calculation on the interface of two blocks. It can model continuous and discontinuous deformation and kinetic characteristics, as well as the asymptotic process from continuum to discontinuum. It also includes block and contact models. The block model consists of a linear elastic model, a plastic model, a block cutting model, a Drucker–Prager model, a Mohr–Coulomb model, a failure model, and a Creep model. The contact model consists of a linear elastic model, a brittle fracture model, a strain softening fracture model, and a fracture flow model. CDEM has been widely used in numerical calculations regarding geotechnical engineering, mining engineering, structural engineering, water resources, and hydropower engineering.

3.1.3.2 The Conditions of Numerical Model
The strata were summarized as three sections: upper-stratum, weak strata, and bedrock. As illustrated in Fig. 9 (Table 2). The rear, front, and bottom of the slope were restricted by displacement, according to Sect. 2.2.1. The pressure on the rear of the slope was

Fig. 6 Landslide shape and monitoring point location about the east open pit mine

Fig. 7 Profile of the physical model experiment about the east open pit mine

0.3 Mpa, and the water pressures near to the F68 fault and crack I were 400 Kpa and 0, respectively. Furthermore, between the F68 fault and crack I, the water pressure was linearly distributed.

3.1.4 The Analyzing of the Numerical Simulation Result

Numerical simulation revealed that the soil near the F68 fault was first damaged under the water pressure.

Fig. 8 The processing of the landslide of the east open pit mine

Fig. 9 Calculation section of numerical simulation about the east open pit mine
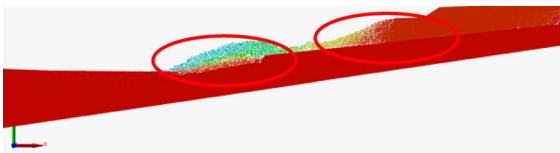
Fig. 10 Fragmented flowing failure and retrogressive cracks about the east open pit mine

The soil and water mixture was then crushed out of the upper-stratum. Finally, the fragmented flowing failure occurred below the F68 fault under the conditions of continuing water supply. Simultaneously, retrogressive cracks occurred on the F68 fault because of the discharge of the lower-stratum soil, as illustrated in Fig. 10. All of the phenomena mentioned above are approximately consistent with the actual landslide.

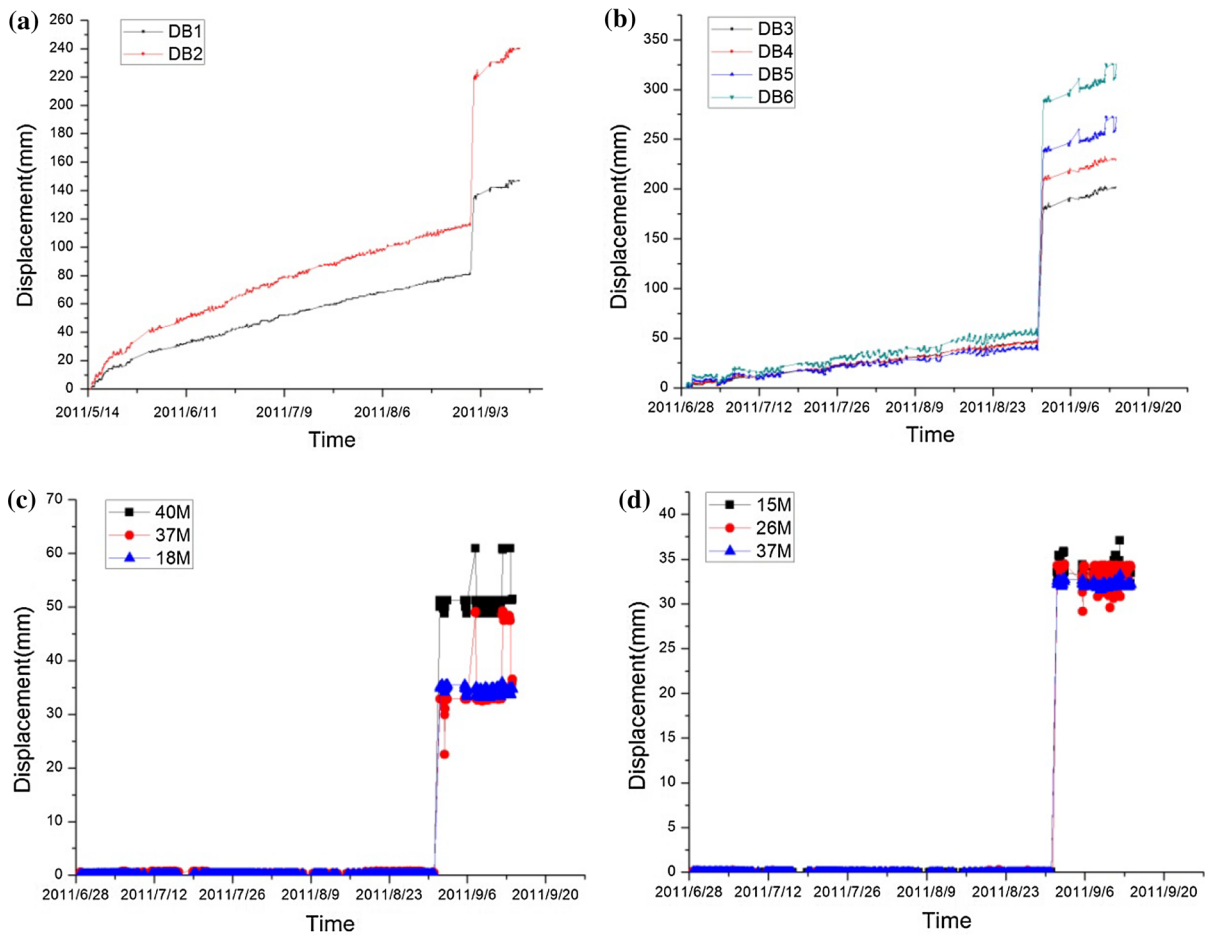### 3.2 Surface and Deep Displacement Monitoring About the North Open Pit Mine

Surface displacement monitoring point DB1, DB2 started from May 14, 2011 to September 14, 2011, and monitoring point DB3, DB4, DB5, DB6, deep displacement monitoring point SB1, SB2 started from June 28, 2011 to September 14, 2011 on the east slope of the north open pit mine (Fan et al. 2013). On August 31, 2011, the landslide occurred following a rainstorm

in north open pit mine, the data of surface and deep displacement both increased rapidly, as illustrated in the Fig. 11a–d. Figure 11c suggested that one relative sliding plane above the 18 m was obtained, dislocation distance was 35 mm, and the other relative sliding plane between 37 and 40 m was obtained, dislocation distance was 20 mm, simultaneously, there was a sliding plane above 15 m according to the Fig. 11d. Based on the above analyzing, the sliding plane was above 15 m, in other words, the sliding plane was in the sand strata, this is a shallow landslide.

3.3 IBIS-M Monitoring Data Analyzing About the North Open Pit Mine

Because of the long term deformation, displacement monitoring of the whole north open pit mine was implemented adopting IBIS-M equipment, equipped with the technology of stepped frequency-continuous wave, synthetic aperture radar, and interferential survey. As illustrated in the Fig. 12, red color represented the deformation towards the equipment, and blue color represented the deformation away from the equipment. The area of blue color circled by the yellow ellipse represented a landslide occurred several years ago. From the Fig. 13, displacement continued to increase with time from May 25, 2011, the maximum displacement of the monitoring point

Fig. 11 Surface and deep displacement monitoring data of the north open pit mine. **a** Surface displacement. **b** Surface displacement. **c** Deep displacement. **d** Deep displacement

reached 0.6 m in fifteen days, according to the investigation of the crack distribution and crack orientation, hazardous area was designated, selected area by yellow line was the landslide occurred on the August 31, 2011.

3.4 Feasibility of the Scheme and Verification

Based on the geological investigation, physical model experiment, and numerical simulation results, a check dam scheme was suggested against the flowing failure in the east open pit mine, including the location, type, size, and construction program. The location of the check dam was across the F68 fault, because water could be drained here as quickly as possible by a drainage system. The check dam was previously built

between the F68 fault and crack I. This region was a severe deformation zone, so the construction of the check dam previous could not be ultimately fulfilled.

The cross section of the check dam is a trapezoid, and now the design height was 40 m. The foundation of the check dam was built on the top of the lower-stratum (elevation 895 m) which is at the bottom of the aquifer according to the borehole data. The construction of the check dam will be fulfilled before next year's rainy season according to the opinion of geological experts.

Compared with the east open pit mine, the mechanism of the north open pit mine was relatively simple, and the depth of the landslide was shallow, so draining wells carried out in 2011 ensured the stability of the slope.

Fig. 12 IBIS monitoring data of the north open pit mine
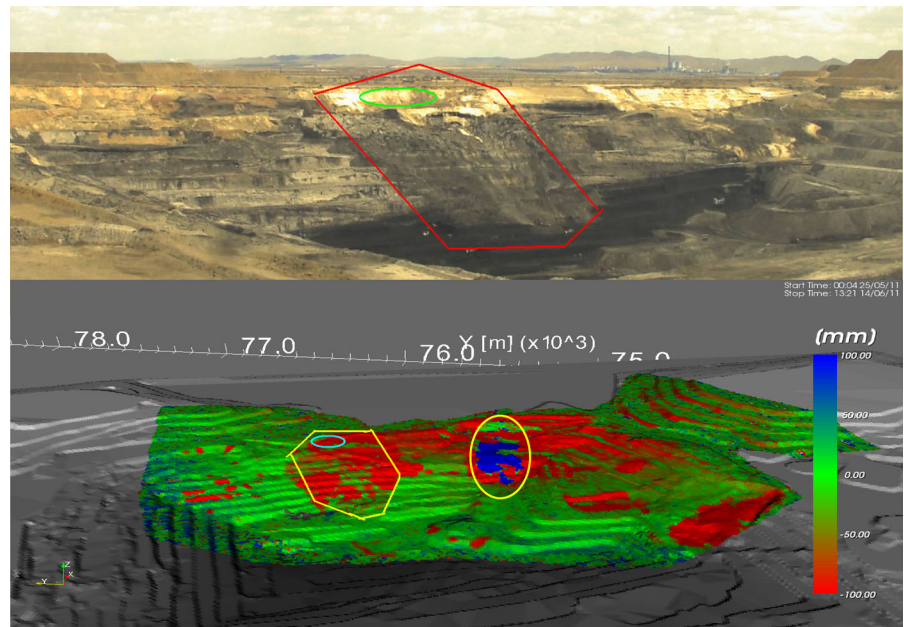
Fig. 13 The curve of displacement versus time about the landslide area
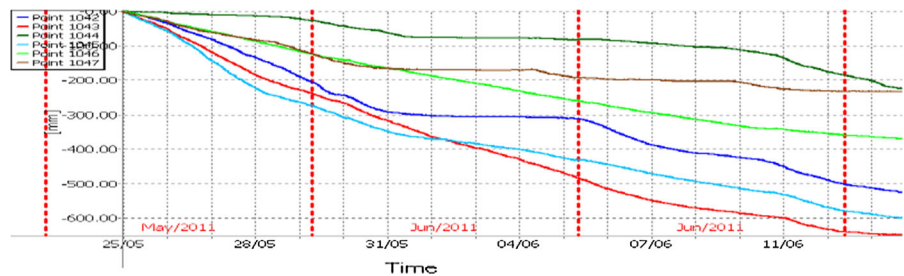
4 Conclusions

The long-term, large displacement and huge volume characteristics landslide of the east open pit mine differed from the traditional landslide. There was not a specific sliding surface, once water concentrated on the F68 fault, soil and water mixture would crush out of the upper-stratum and form the fragmented flowing failure. The landslide of the north open pit mine belonged to the traditional shallow landslide. In summary, some of the conclusions obtained are as follows:

1. Based on the geological investigation, the total volume of the east open pit mine landslide was nearly 85 million m^3 (on August 16, 2013). From 2011 to the present, five landslides occurred that were connected with the state and migration characteristics of groundwater as well as the permeability of fault F68. The total volume of the north open pit mine landslide was nearly 1 million m^3 (on August 31, 2011). From 2005 to 2011, five landslides occurred that were connected with the rainstorm.

2. As a whole, the east open pit mine landslide was divided into two parts. Below the fault F68, the failure process of the slope was summarized as (a) water accumulation, (b) fragmented destruction, and (c) flowing; upon the fault F68, retrogressive failure occurred because of discharge of the lower-stratum soil. If no measures were taken, the landslide would not stop until the slope was flat.

3. According to the characteristics of the east open pit mine landslide, a check dam location above the fault F68 was determined. Water could be drained here as quickly as possible by a drainage system.

116 draining wells carried out in 2011 ensured the stability of the north open pit mine landslide. Simultaneously, the management of seepage water effectively avoided the soaking of the mudstone strata. The lessons learned from the two landslides may be valuable for the understanding of the mechanism of landslides and improving preventative measures against these types of events in north China in the future.

References

Acharya G, Cochrane TA, Davies T (2009) The influence of shallow landslides on sediment supply: a flume-based investigation using sandy soil. Eng Geol 109:161–169

Chanson H (2004) Sabo check dams-mountain protection systems in Japan. J River Basin Manag 2(4):301–307

Cruden DM (1991) A simple definition of landslide. Bull Int Assoc Eng Geol 43(1):27–29

Cuomo S (2014) New advances and challenges for numerical modeling of landslides of the flow type. Procedia Earth Planet Sci 9:91–100

Fan YB, Hou YF, Li SH (2013) Landslide stability analysis based on surface and deep displacement monitoring data. J Eng Geol 21(6):885–891

Feng C, Li SH, Liu XY, Zhang YN (2014) A semi-spring and semi-edge combined contact model in CDEM and its application to analysis of Jiweishan landslide. J Rock Mech Geotech Eng 6(1):26–35

Hitoshi S, Daichi N, Hiroshi M (2010) Relationship between the initiation of a shallow landslide and rainfall intensity-duration thresholds in Japan. Geomorphology 118:167–175

Huang CC, Chien LL, Jang JS (2008) Internal soil moisture response to rainfall-induced slope failures and debris discharge. Eng Geol 101:134–145

Li SH (2013) Progressive failure constitutive model of fracture plane in geo-material based on strain strength distribution. Int J Solids Struct 50(3–4):570–577

Pánek T (2013) Holocene reactivations of catastrophic complex flow-like landslides in the Flysch Carpathians (Czech Republic/Slovakia). Quat Res 80:33–46

Qi SW, Yan FZ, Wang SJ (2006) Characteristics, mechanism and development tendency of deformation of Maoping landslide after commission of Geheyan reservoir on the Qingjiang River, Hubei Province, China. Eng Geol 86:37–51

Qu YZ, Hao ZD, Bao JM (2009) Stability analyzing about south working slope in Shengli open- pit mine. Opencast Min Technol 02:16–22

Shu JS (2009) The slope stability analyzing and controlling about the ShengLi east open pitmine, 1–15 **(in Chinese)**

Sun XH, Shu JS, Guo BB (2008) Probing into eastern working slope south part landslide mechanism in Shengli open- pit mine. Opencast Min Technol 04:14–16

Varnes DJ (1958) Landslide types and processes. Highway research board special report, vol 29, pp 20–47

Varnes DJ (1984) Landslide hazard zonation: a review of principles and practice. Nat Hazards 3:1–56

Wang GL (2013a) Lessons learned from protective measures associated with the 2010 Zhouqu debris flow disaster in China. Nat Hazards 69:1835–1847

Wang LX (2013b) A GPU-based parallel procedure for non-linear analysis of complex structures using a coupled FEM/DEM approach. Math Probl Eng 61(8):1–15

Wang GL (2014) Comparison of the landslides triggered by the 2013 Lushan earthquake with those triggered by the strong 2008 Wenchuan earthquake in areas with high seismic intensities. Bull Eng Geol Environ. doi:10.1007/s10064-014-0574-z

Wang GH, Sassa KJ (2003) Pore-pressure generation and movement of rainfall-induced landslides: effects of grain size and fine-particle content. Eng Geol 69:109–125

Wang J, Li SH, Zhang QB (2015) Simulation of crack propagation of rock based on splitting elements. Chin J Theor Appl Mech 47(1):1–14

Zeng QL, Yue ZQ, Yang ZF, Zhang XJ (2009) A case study of long-term field performance of check-dams in mitigation of soil erosion in Jiangjia stream, China. Environ Geol 58:897–911

Zhou JW, Xu WY, Yang XG et al (2010) The 28 October 1996 landslide and analysis of the stability of the current Huashiban slope at the Liangjiaren Hydropower Station, Southwest China. Eng Geol 114:45–56